Geosynthetics in unpaved roads on soft subgrade: Large-Scale Experiments and numerical approach

N. Khoueiry
WSP, F-75012, France (nicole.khoueiry@wsp.com)

L. Briançon
University of Lyon, INSA Lyon, GEOMAS, F-69621, France (laurent.briancon@insa-lyon.fr)

M. Riot
AFITEXINOV, F-28300, France (mathilde.riot@afitex.com)

A. Daouadji
University of Lyon, INSA Lyon, GEOMAS, F-69621, France (ali.daouadji@insa-lyon.fr)

ABSTRACT: The geosynthetics were used in unpaved roads on soft subgrade since 1970. However, the developed mechanisms in unpaved reinforced roads are complex. To clarify and identify these mechanisms a full-scale laboratory test has been developed. An unpaved reinforced or unreinforced tested platform has been constituted in a laboratory large geotechnical box. The prepared platform was subjected to a cyclic plate load of a maximum magnitude of 40 kN resulting in a surface pressure of 560 kPa. The platform was subjected to 10,000 cycles. Two base course platforms were tested (350 and 220 mm). A knitted geogrid was used in the reinforced platforms. A special attention was given to the soil layers composition, installation, and compaction. The test repeatability was checked. The experimental results showed the geosynthetic benefits in the platforms with a base course thickness of 220 mm. However, for a base course thickness of 350 mm the geosynthetic was not effective. A numerical model was developed using the software FLAC 3D® to simulate the structure behavior under the first applied load. The results showed that the numerical model captures the structure behavior for the reinforced and unreinforced platforms.

1 INTRODUCTION

Along these years, the experience proved the efficiency of the geosynthetic in increasing the load support capacity and the serviceability of the unpaved roads structures.
From the very early geosynthetics applications in unpaved road reinforcement, it is been shown that the reinforcement can reduce the base coarse fill material thickness about 30% (Cancelli and Montanelli, 1999; Miura et al, 1990l; Watts and Brady, 1990).
The previous studies highlighted the effect of the geosynthetic. In fact, Bloise and Ucciardo (2000) noted that the reinforcement presence facilitates the aggregate platform compaction. Floss and Gold (1994), Huntington and Kasibati (2000) and Meyer and Elias (1999) reported that the geosynthetics improve the platform bearing capacity. Bloise and Ucciardo (2000), Huntington and Kasibati (2000), Cancelli and Montanelli (1999); Jenner and Paul (2000), Martin (1988) and Miura et al (1990) concluded that the geosynthetic allow the reduction of the granular platform thickness. Meyer and Elias (1999), Cancelli and Montanelli (1999) and Knapton and Austin (1996) reported the effect of the geosynthetic on the rut development delay
The structure heterogeneity, and the various factors and parameters that affect the structure response result in the fact that there are no clear and general design method for this structure. This clearly highlights the need of further investigations in this field.

In this study, a large-scale laboratory test was developed to quantify the efficiency of the geosynthetic in this application and provide more knowledge regarding the developed mechanisms at the interface between the geosynthetics and the granular platform.
In this paper, the large scale developed experiment is presented and detailed. The results of the experimental plate load test were compared to the numerical results of a developed differential element method model.

2 BACKGROUND

The unpaved road composed of a soft subgrade supporting a rigid aggregate platform is a complex structure subjected to traffic load. The reinforcement of the base course platform complicates even more the behavior of the structure.

In fact, two mechanisms take place at the reinforcement interface:

(1) The stabilization mechanism: The base course platform confinement, which is provided by the interlocking mechanism with a geogrid, and the friction mechanism with a geotextile. In fact, the interlocking and friction mechanisms reduce the aggregates lateral displacement under the load, which increases the base course stiffness and the load distribution angle. Hence, the vertical stress on the subgrade surface decreases.
(2) The reinforcement mechanism: The ability of the geosynthetic sheet to be deformed and to absorb the vertical load initially perpendicular to its surface, this is called the membrane effect reinforcement mechanism. The more the geosynthetic sheet is deformed the more the membrane effect is efficient. In the earliest studies regarding this application, the tension membrane effect was considered as the most reinforcement contributor mechanism (Giround and Noiray, 1981). However, most recent studies reported the important contribution of the confinement mechanism (Giroud, 2009; Giroud and Han, 2004; Cook et al, 2016).

The dominance of the stabilization and reinforcement mechanisms, depends on the properties and thickness of the base course, the subgrade properties, the position, the layers number, the stiffness, the type, and the maximum tension strength of the geosynthetic. In addition, in the case of a geogrid the apertures form and dimensions, the joints and ribs stiffnesses are added to the list of influencing parameters.
In literature, different authors used physical and numerical approaches to study the influence of different parameters: the optimum geosynthetic position (Cancelli and Montanelli, 1999; Walters et al, 2002; Akond, 2012), the effect of geogrid aperture shape (Qian et al, 2011; Qian et al, 2013; Dong et al, 2010), the geogrid aperture size (Szatmari, 2016; McDowell et al, 2006; Brown et al, 2007) and the geogrids ribs stiffness (Giroud, 2009; Qian et al, 2013; Brown et al, 2007; Hufenus et al, 2006; Sun et al, 20015).
Advanced and developed numerical models were used in literature to simulate the geosynthetic behavior and impact. Berrabah et al (2020) used a 3D FE model to study the influence of the reinforcement, also to demonstrate the effect of 3D modeling on the settlement. Leonardi et al (2020) used a 3D FE model to analyze the improvement in terms of rutting reduction of a reinforced unpaved road. However, the use of continuum-based finite or differential element methods reduces the geosynthetic/aggregates interface complex behavior to an elasto-plastic shear law. Therefore, still no reliable continuum-based model and clear calibrated parameters can simulate the reinforced effect in this application.
To compare the effect of all these affecting parameters and provide additional knowledge regarding the stabilization/reinforcement mechanisms, a large-scale laboratory test was developed and is presented in this paper. Moreover, a discrete element 3D model was calibrated and developed on the base of the physical model.

3 EXPERIMENTAL DEVICE

The cyclic plate load tests were performed on an unpaved platform placed in a box of 1.8 m of large, 1.9 m of length and 1.1 m of height. The platform was constituted of 350 or 220 mm of base course overcoming 600 mm of soft soil. The test consisted of applying a cyclic load using a 300 mm diameter rigid plate on the surface of an unpaved road supported by a soft subgrade. The maximum load applied at the platform surface was 40 kN, equal to the half-axle load (ESAL: Equivalent Single Axle Loads) based on the American standard (AASHTO, 1993), with an applied pressure of 566 kPa.
The cyclic load was applied at a constant frequency no greater than 1 Hz as specified in [32]. The cycle load was generated by a hydraulic loading system as seen in Figure 1. The unpaved road tested with this facility are supposed to support 10,000 ESAL passes, with a maximum rutting of 75 mm regarding (FHWA, 2008).

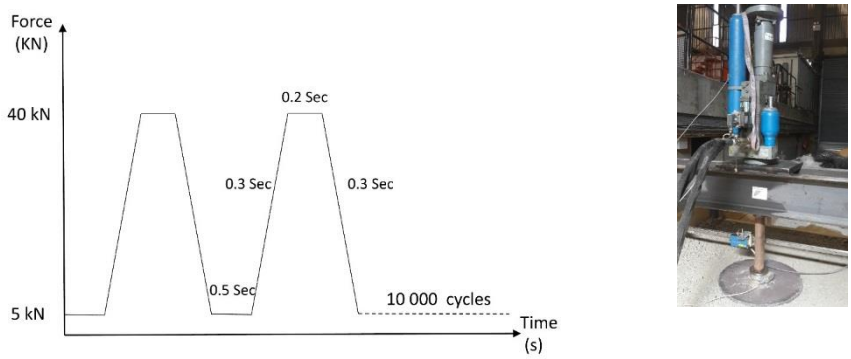

Figure 1. (a) Load waves diagram, (b) Hydraulic Jack.

4 MATERIALS

Figure 2 illustrates the soil layers constitution and the position of the GSY (Geosynthetic) in the plate load test. The CBR of the soft subgrade should be less than 3% so a GSY reinforcement is in need regarding FHWA (2008) . standard. The CBR required for the granular platform is 20% (FHWA, 2008). In the plate load test, two granular platform thicknesses were tested, 350 mm and 220 mm.
A light non-woven geotextile was placed at the interface between the soft subgrade layer and the base course layer to reduce the pollution of the two different layers, especially that the same soils are reused in the different constitutive tests.

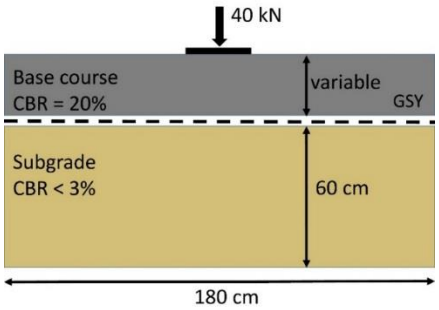

Figure 2. Platform soil layers constitution.

4.1. *Soft subgrade*

To simulate the same subgrade with the same properties for each prepared laboratory test an artificial subgrade was constituted of a clay and sand mixture. A mixture of 20% Kaolinite clay and 80% of Hostun sand was chosen to simulate the subgrade soil. The proctor tests showed that the compaction of this mixture at 11% of water content gives a soil layer with a CBR of 2%.

4.2. *Aggregates*

The aggregates used in these tests are non-treated aggregates with particles diameters ranging between 0 and 31.5 mm. The proctor tests showed that the optimum proctor dry density is reached at 4% of water content.

4.3. *GSYs*

The tested geosynthetic is a knitted coated geogrid with a square shaped aperture. The aperture dimension is 40 mm. The maximum tension strength is equal in both directions to 100 kN/m and the geogrid stiffness at 2% of strain is equal 1000 kN/m.

5 INSTRUMENTATION

The test was instrumented with Earth Pressure Cells (EPC), settlement sensors (S), displacement laser sensor, inclination sensors (I), and fibre optic sensors. To monitor the vertical stress distribution on the subgrade surface in the plate load test, five earth pressure cells were placed in different locations from the plate load centre (Figure 3). Moreover, earth pressure cells were placed in different depth positions under the plate load centre, at 200 mm, 400 mm and 600 mm of the subgrade depth. Five settlement sensors were placed in different positions at the subgrade surface to monitor the surface displacement during cycles. The displacement laser sensor was used in order to monitor the plate displacement over the cycles. Fibre optic sensors were placed in the GSY to measure the strain developed in the reinforcement during the loading. The spread sensor technology was used in this application, and the results analysis is based on the principle of measuring Rayleigh backscatter (Optical Frequency Domain Reflectometry). This optical system is able to measure and acquire strain with a spatial resolution as high as 0.65 mm, providing highly detailed mapping of strain profiles.

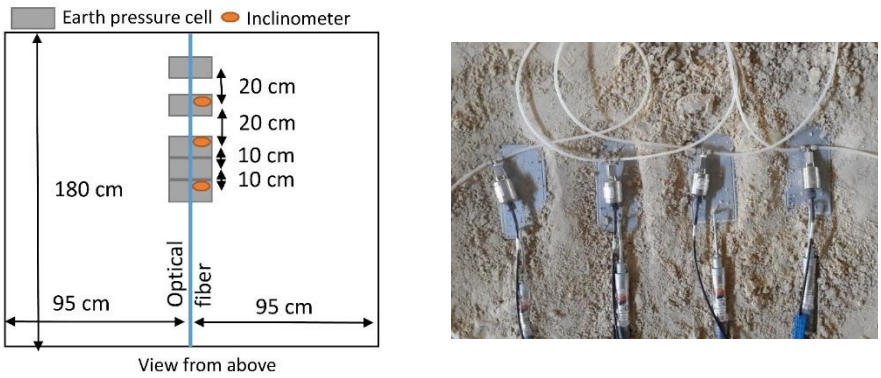

Figure 3. Platform instrumentation in the plate load test, view from above.

6 TEST SETUP

The main aim at this stage was to find a good installation protocol in order to obtain a homogeneous layer in depth and the overall area with a CBR ratio of 2% for the soft subgrade and 20% for the fill material. Therefore, a series of installation tests were performed, and for each test, the quality control tests were performed to control the installed soil properties and homogeneity. The adapted installation protocol consisted of:

- Placing the first 200 mm, which corresponds to 1,400 kg of subgrade soil. This layer is not subjected to any compaction since it will be subjected to the overall compaction of the soil above.
- Placing 100 mm of soil, which corresponds to 700 kg of subgrade soil. This layer is subjected to one plate compactor pass. This step was repeated three times over three layers of 100 mm.
- Placing the last 100 mm of subgrade without compaction since it will be affected by the aggregates compaction.
- Placing the first 110 mm of aggregates, which corresponds to 800 kg of aggregates. This layer is subjected to four compactor passes. Another aggregates layer of 110 mm was placed with the same procedure.

7 PERFORMED TESTS

The base course thickness effect was studied by performing tests with reinforced and unreinforced platforms and two base course thicknesses (350 and 220 mm). The main aim of these tests is to compare the geogrids platform improvement effect. In order to allow the comparison, the test repeatability should be insured. Therefore, two identical tests were performed for the unreinforced platform, the reinforced platform with the geogrid described previously (GSY). The performed tests are resumed Table 1.

Table 1. Performed tests details.

Test number	Base course thickness (mm)	Reinforcement	GSY position	Test status
Test 1	350	Unreinforced		Reference test
Test 2	350	GSY	Interface	GSY improvement test
Test 3	220	Unreinforced		Reference test
Test 4	220	Unreinforced		Repeatability test
Test 5	220	GSY	Interface	GSY improvement test
Test 6	220	GSY	Interface	Repeatability test

8 QUALITY CONTROL TESTS

The quality control tests are performed on each prepared platform, in order to make sure that for each performed test the soil layers have the same properties and are under the same conditions. The water content was measured in depth for each prepared subgrade. Static

penetrometer was used too in the subgrade soil to determine the cone index, which is correlated to the CBR (%) by the apparatus manufactural. The dynamic cone penetrometer was performed on the subgrade soil before the base course installation and after the base course installation to control the base course and the subgrade CBR (%). The correlated CBR profiles showed that the installation protocol provides homogeneous soil layers with the required CBR values and confirmed the platforms properties repeatability.

9 EXPERIMENTAL RESULTS

During the tests, the subgrade and the base course surface displacement and the vertical stress distribution on the subgrade were monitored.

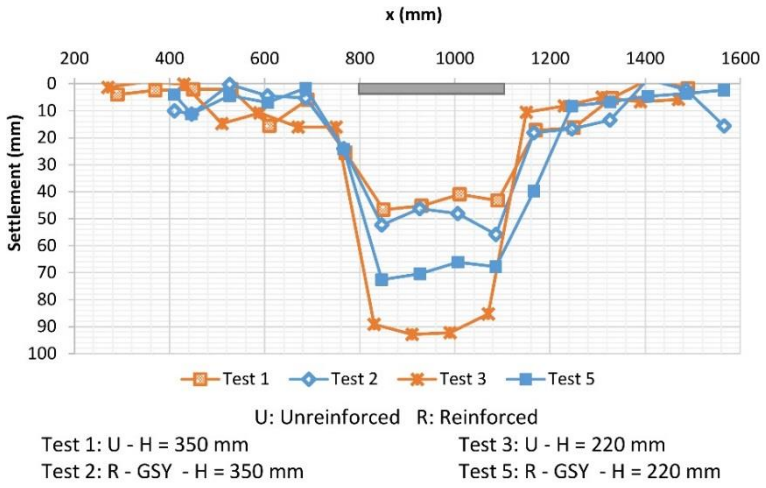

Figure 4. Base course surface settlement after 10,000 cycles.

Two tests were performed with a base course thickness of 350 mm, one with reinforcement (Test 2) and another without reinforcement (Test 1). The results show that the reinforcement placed at the interface effect can be negligible for a base course thickness of 350 mm. In fact, Figure 4 shows a small difference in final rutting for H = 350 mm between a reinforced and an unreinforced platform.

Identical tests were performed to check the experimentation repeatability. In fact, in order to compare the results, the test repeatability should be checked especially in such large-scale test. Tests 3 & 4 are the identical unreinforced tests with H = 220 mm, Tests 5 & 6 are the identical reinforced with GSY and H = 220 mm. The maximum central subgrade settlement evolution with cycles for the identical performed tests is shown in Figure 5. It shows close displacement results given by each two identical tests, which proved the tests repeatability.

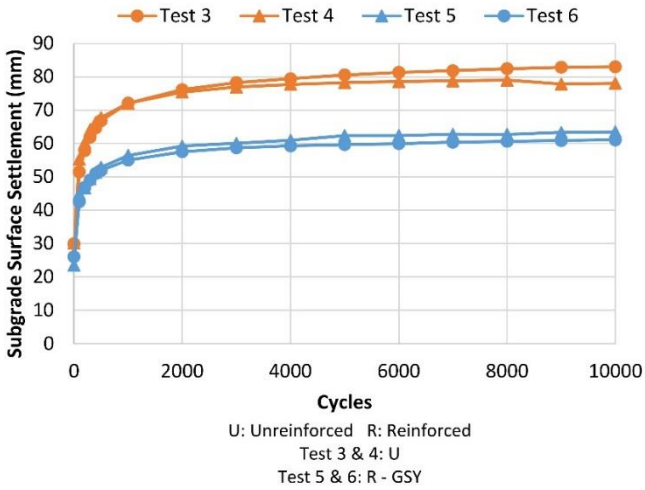

Figure 5. Base course surface center settlement evolution with cycles (for H = 220 mm).

Moreover, Figure 4 and Figure 5 show the subgrade settlement reduction given by the reinforcement after 10,000 cycles. In fact, the central base course surface settlement after 10,000 cycles, is 80 mm for the unreinforced platform and 60 mm for the reinforced platforms. Which shows that the reinforcement reduced the final rutting of about 25%.

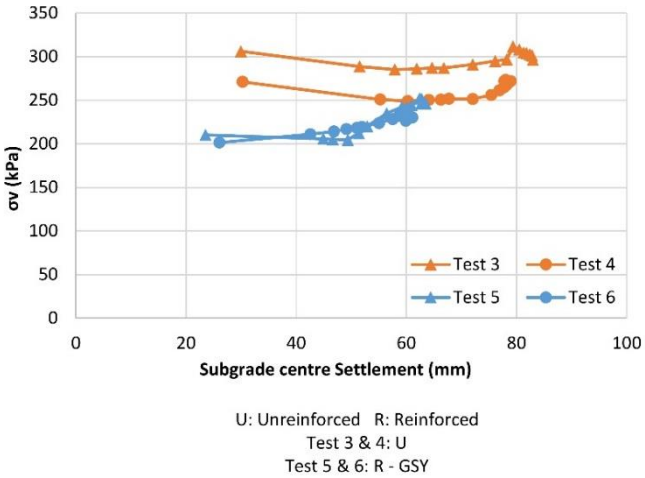

Figure 6. Subgrade surface central vertical stress evolution with settlement (for H = 220 mm).

Figure 6 shows the stress evolution with settlement at the same position, which is the subgrade surface centre. The unreinforced platform (Test 3 & Test 4) shows a high settlement at the first cycles with the highest stress magnitude of 300 kPa, and over the cycles, the settlement increases over an important rate due to the subgrade damage under the cyclic load. This graph shows clearly that the reinforcement presence reduces the maximum stress applied at the subgrade surface, which resulted in the reduction of the rut development.

10 NUMERICAL MODEL

FLAC 3D is a software based on differential element method and was used to simulate the first applied load on the reinforced and unreinforced platforms. Due to the symmetry, only the quarter of the domain is modelled. The quarter of a cylinder with a radius of 900 mm represents the quarter soil layers with 600 mm of subgrade and 220 mm of base course. Two different simulations with and without reinforcement were performed in order to compare the reinforcement effect. The boundary conditions are imposed regarding the symmetry and the physical model. In fact, the displacement in the z direction at the bottom face and the displacement in the normal directions of the model lateral faces were blocked.

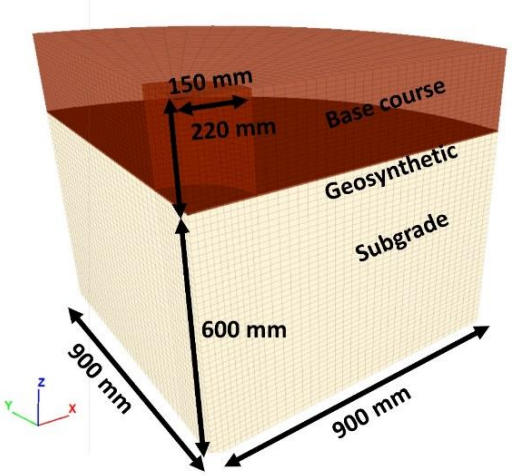

Figure 7. The model geometry.

10.1. *Materials Parameters*

10.1.1. Subgrade

The Cap-yield constitutive model implemented in FLAC was used to illustrate the subgrade behaviour, a shear and volumetric hardening/softening model that can simulate the nonlinear behaviour of the soil.
The model was calibrated based on a monotonic triaxial test. An undrained experimental test was performed on an unsaturated soil (soil at 72% of saturation). The experiments give the apparent cohesion (CUU) of 19 kPa and the apparent friction angle (φUU) of 28° of the unsaturated soil. However, in the numerical simulations the soft soil is assumed to be a dry soil. The apparent behaviour of the unsaturated soil was used to calibrate the behaviour of the dry soil in the numerical simulations. The parameters given in Table 2 are the final parameters that gave the matching numerical and experimental curves.

Table 2. Subgrade Cap-Yield Model calibrated properties.

Density (kN/m^3)	19	Failure ratio Rf	0.9
Elastic bulk modulus K (MPa)	57.5	Ultimate friction angle φ_f (°)	28
Elastic shear modulus G (MPa)	26.5	Calibration factor β	0.3
Poisson's ratio υ	0.3	Shear reference	200
friction angle φ (°)	28	Critical friction angle (°)	19
dilation angle Ψ (°)	5	Pressure-reference (kPa)	100
cohesion C (kPa)	19	Exponent m	0.99

10.1.2. Base course

The base course material used in the physical model was characterized using a large shear box test. To simulate the same base course performances in the numerical model, a numerical shear

box test was performed. The Mohr-Coulomb constitutive model was used for the base course material. Table 3 shows the used parameters.

Table 3. The base course Mohr-Coulomb Model calibrated properties.

Density (kN/m^3)	18	friction angle φ (°)	37
Elastic bulk modulus K (MPa)	125	dilation angle Ψ (°)	15
Elastic shear modulus G (MPa)	58	cohesion C (kPa)	10
Poisson's ratio ν	0.3		

10.1.3. GSY

The geogrid is simulated as a membrane characterized by an elastic behavior in its plane. The experimental tests used to verify the numerical simulation are the ones conducted using GSY as a reinforcement: a knitted coated geogrid with 1,000 kN/m as stiffness at 2% of strain. The membrane thickness is taken equal 3 mm, so the young modulus is taken equal the geogrid stiffness expressed in kN/m divided by the membrane thickness and is equal 333 MPa. The Poisson's ratio was taken equal 0.33.

10.1.4. Base course/Geosynthetic interface

A numerical shear box test was performed with geosynthetic placed at the interface. The Mohr-Coulomb constitutive model was used for the geosynthetic interface. The shear stiffness was taken equal to 360 MPa, the cohesion equal 15 kPa and the friction angle equal 39°.

10.1.5. Base course/Subgrade interface

The interfaces provided by FLAC are characterized by Coulomb sliding and/or tensile separation. FLAC manual recommends a method to determine the interface stiffness in the case of contact between a material much stiffer than the other. This method considers that the Ks and Kn should be taken equal ten times the equivalent stiffness of the softer neighboring zone. The normal and shear stiffnesses were taken equal 9.28 MPa, the friction angle equal 28° and the cohesion equal 19 kPa.
To understand the influence of these calibrated parameters on the numerical results a numerical parametric sensitivity was performed and is presented in the thesis manuscript (Khoueiry, 2020). This parametric study showed that:

- The base course friction angle presents a major effect, while the base course elastic modulus presents a minor effect,
- The interface base course/geosynthetic parameters presents a minor effect,
- The reinforcement stiffness presents an important effect on the maximum subgrade stress reduction.
- The base course thickness affects the most the vertical stress distribution,
- The subgrade/base course interface properties present no influence on the stress distribution.

11 NUMERICAL AND EXPERIMENTAL COMPARISON

A monotonic displacement was applied in this case on the top surface of the base course and the results were compared to the first load application results obtained from the experimental tests. In the numerical simulations, a displacement rate was applied until the average vertical stress at the surface reaches 560 kPa. This simulation was conducted for a reinforced and unreinforced case with a base course thicknesses of 220 mm. The simulation was resolved as a large-strain problem, in which the coordinate new positions are calculated and updated for each step.
The settlement profile on the subgrade surface is plotted and compared to the experimental settlement results in Figure 8. Under the plate center line for the reinforced model, numerically

the settlement is about 24 mm, experimentally 26 mm. For the unreinforced model, numerically the settlement is about 28 mm, experimentally 30 mm. By comparing the reinforced and unreinforced center line settlement results, it can be noted that the reinforcement reduces the central settlement of 13% in both numerical and experimental models under monotonic load. Figure 9 shows the comparison between the reinforced and unreinforced experimental and numerical vertical stress distributions on the subgrade surface. For the unreinforced platform, close results are observed between the experimental and numerical stresses at the plate centre, and at a distance of 200 mm and 300 mm from the plate centre line. In fact, at the plate centre, the numerical and experimental vertical stress is about 306 kPa.

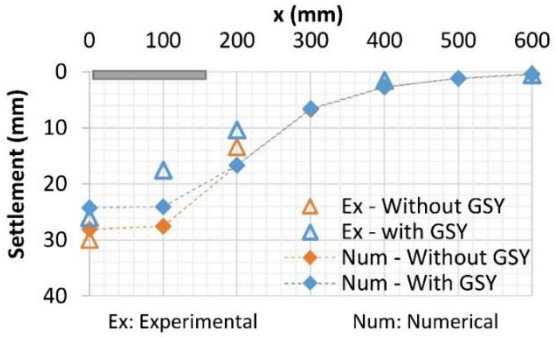

Figure 8. Subgrade surface settlement for the reinforced and unreinforced numerical and physical models with a platform thickness of 220 mm.

For the reinforced platform a difference between the experimental and numerical results is observed particularly under the plate. Indeed, the numerical vertical stress at the plate centre line is equal 242 kPa, the experimental vertical stress is 200 kPa. However, for the reinforced and unreinforced platforms, the numerical and experimental vertical stresses tend to zero between 300 and 400 mm from the plate centre. These slight differences can be due to local interface phenomenon between the aggregates and the geogrid apertures that are not perfectly simulated in this model and to the stress measurements uncertainties.

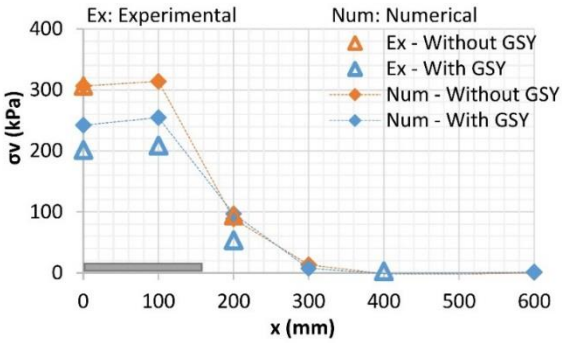

Figure 9. Subgrade surface vertical stress distribution for the reinforced and unreinforced numerical and physical models.

Figure 10 shows a comparison between the numerical and the experimental developed force in kN/m in the geosynthetic. In fact, experimentally the GSY deformation was measured using the fibre optic sensor and knowing the GSY stiffness the developed force in the GSY was calculated.

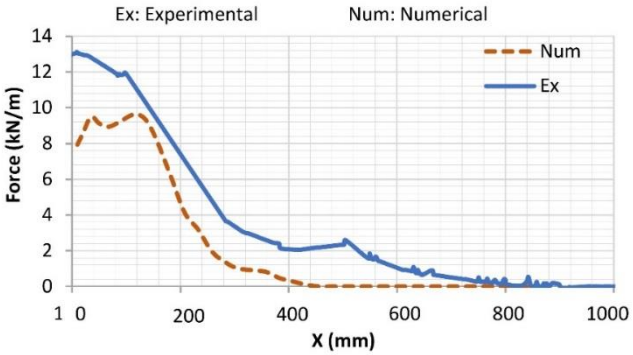

Figure 10. Force in kN/m developed in the geosynthetic in the numerical and physical model.

Figure 10 shows a match between the experimental and numerical developed force. It can be seen that the numerical simulation underestimates the developed force. Indeed, the average maximum developed force numerically the geosynthetic is 10 kN/m and experimentally 12 kN/m. Moreover, the geosynthetic presents experimentally a larger area of tension than the numerical case. These differences can be due to the interface aggregates and geogrid apertures interaction that is reduced in this model to a simple shear law.

12 CONCLUSIONS

In this paper, the developed protocol to test the unpaved roads under cyclic plate load was detailed, and the first performed tests results were presented. The reinforced and unreinforced platforms with 350 mm showed that the GSY placed at the interface in the case of a thick base course layer has a limited effect on the reinforced platform. However, the performed tests with the base course thickness of 220 mm showed the benefits of the reinforcement. In fact, the reinforcement reduced the surface settlement of about 25 %. Moreover, the repeatability tests performed proved the test protocol repeatability.
The continuous-based differential element method with the software FLAC 3D was used to simulate the behaviour of this structure under the first applied load. Reinforced and unreinforced platforms were simulated with 220 mm of base course thickness and compared to the first cycle of the experimental reinforced and unreinforced results. The numerical and experimental displacement curves showed that the numerical model can capture the experimental soft soil displacement. Moreover, the stress distribution on the soft subgrade surface was predicted by the numerical model. Differences were shown in the stress values especially in the reinforced model, but it can be assigned to the inaccurate stress measurements in a soft soil. The comparison between the numerical and experimental geosynthetic developed force showed that the numerical model can predict the reinforcement behaviour. The comparison between the reinforced and unreinforced numerical results showed the effect of the reinforcement in reducing the maximum vertical stress on the subgrade, which reduced the surface settlement. It is worth pointing out that, in this model, the non-linear behaviour of the base course related to the grains rearrangements is not taken into consideration. Moreover, the base course/geosynthetic interface is reduced to an elastic perfectly plastic behaviour. More developed model regarding the aggregates behaviour and the interlocking mechanism is needed to better investigate the interface behaviour and the lateral movement of the aggregates under the load.

REFERENCES

AASHTO (1993) AASHTO Guide For Design Of Pavement Structures. II–69.

Akond, I. (2012) Laboratory Evaluation of Geosynthetics to Stabilize/Reinforce the Subgrade/Base in Unpaved Roadways

Berg, R. R. (2000) Geosynthetic Reinforcement of the Aggregate Base/Subbase Courses of Pavement Structures

Berrabah, F., Benmebarek, S. and Benmebarek, N. (2020) Three-dimensional numerical analysis of geosynthetic-reinforced embankment over locally weak zone. *Transportation Infrastructure Geotechnology,* **7**, 269-296

Bloise, N. and Ucciardo, S. (2000) On site test of reinforced freeway with high-strength geosynthetics *Eurogeo 2000,* **1**

Brown, S. F., Kwan, J. and Thom, N. H. (2007) Identifying the key parameters that influence geogrid reinforcement of railway ballast, *Geot. and Geom.,* **25**, 326 335.

Cancelli, A. and Montanelli, F. (1999) In-ground test for geosynthetic reinforced flexible paved roads **2**

Cook J, Dobie M and Blackman D 2016 The development of APT methodology in the application and derivation of geosynthetic benefits in roadway design, *The Rol.of Acc. Pav. Tes. in Pav.t Sust.* 257-275

Dong, Y. L., Han, J. and Bai, X. H. (2010) Bearing capacities of geogrid-reinforced sand bases under static loading *Grou. Impro. and Geos.,* 275-281

FHWA Federal Highway Administration (2008) Geosynthetic design and construction guidelines reference manual FHWA NHI-07-092 U.S. Dept. of Transportation, Federal Highway Administration, Washington DC

Floss, R. and Gold, G. (1994) Causes for the improved bearing behaviour of the reinforced two-layer system *Proc. 5th Int. Conf. Geot., Geom., and Rel. Prod.,* **1,** 147-150.

Giroud, J. P. (2009) An assessment of the use of geogrids in unpaved roads and unpaved areas *Jub. Sym. on poly. Geo. Reinf.*

Giroud, J. P. and Han, J. (2004) Design method for geogrid-reinforced unpaved roads II Calibration and applications *J. of Geot. and Geo. Eng.,* **130**, 787-797

Giroud, J. P. and Noiray, L. (1981) Geotextile-reinforced unpaved road *design J. of Geot.and Geo. Eng.,* **107** ASCE 16489

Hufenus, R., Rueegger, R., Banjacm R., Mayor, P., Springman, S. M. and Brönnimann, R. (2006) Full-scale field tests on geosynthetic reinforced unpaved roads on soft subgrade *Geot. and Geom.,* **24**, 21- 37

Huntington, G. and Ksaibati, K. (2000) Evaluation of geogrid-reinforced granular base *Geot. Fab. Rep.,* **18**

Jenner, C. G. and Paul, J. (2000) Lessons learned from 20 years experience of geosynthetic reinforcement on pavement foundations *Eurogeo 2000,* **1**

Khoueiry, N. (2020) Study of granular platforms behaviour over soft subgrade reinforced by geosynthetics: Experimental and numerical approaches (Doctoral dissertation, Université de Lyon).

Knapton, J. and Austin, R. A. (1996) Laboratory testing of reinforced unpaved roads *Ear.Reinf.* 615 618

Leonardi, G., Lo Bosco, D., Palamara, R. and Suraci, F. (2020) Finite element analysis of geogrid-stabilized unpaved roads, *Sustainability*, **12**, 1929

Martin, D. (1988) Die trennfunktion der geotextilien in ungebundenen verkehrswegebefestigungen *Tag. Kun. in der Geo. Mun.,* **1,** 77-86

McDowell, G. R., Harireche, O., Konietzky, H., Brown, S. F. and Thom, N. H. (2006) Discrete element modelling of geogrid-reinforced aggregates, *Proc. of the Ins. of Civ. Eng. Geot. Eng.,* **159**, 35-48

Meyer, N. and Elias, J. M. (1999) Dimensionierung von Oberbauten von Verkehrsflachen unter Einsatz von multifunktionalen Geogrids zur Stabilisierung des Untergrundes, *Tag. Kun. in der Geo. Mun.,* **6,** 261-268.

Miura, N., Sakai, A., Taesirim, Y., Yamanouchi, T. and Yasuhara, K. (1990) Polymer grid reinforced pavement on soft clay grounds, *Geot.and Geom.,* **9**, 99-123

Perkins, S. W. (2000) Constitutive modeling of geosynthetics, *Geot.and Geom.,* **18**, 273-292

Qian, Y., Han, J., Pokharel, S. K. and Parsons, R. L. (2011) Stress analysis on triangular-aperture geogrid-reinforced bases over weak subgrade under cyclic loading: An experimental study *Trans. Res. Rec.,* **2204,** 183-91

Qian, Y., Han, J., Pokharel, S. K. and Parsons, R. L. (2013) Performance of triangular aperture geogrid-reinforced base courses over weak subgrade under cyclic loading, *J. of Mat. in Civ. Eng.,* **25**, 1013- 1021

Sun, X., Han, J., Kwonm J., Parsons, R. L. and Wayne, M. H. (2015) Radial stresses and resilient deformations of geogrid-stabilized unpaved roads under cyclic plate loading tests, *Geot.and Geom*. **43**, 440-449

Szatmári, T. (2016) Investigation of the geogrid-granular soil combination layer with laboratory multi-level shear box test *Eurogeo 2016*

Walters, D. L., Allen, T. M. and Bathurst, R. J. (2002) Conversion of geosynthetic strain to load using reinforcement stiffness, *Geos. Int.,* **9**, 483 523

Watts, G. R. A. and Brady, K. C. (1990) Site damage trials on geotextiles Four *Int. Conf. on Geot. Geom. and Rel. Pro.,* 603-607